Effect of humidity and gas density on switching impulse breakdown of short airgaps

A.J. Davies, BSc, PhD, CEng, FIEE
Prof. J. Dutton, BSc, PhD, DSc
R. Turri, Dott Ing
Prof. R.T. Waters, BSc, PhD, CEng, FIEE

Indexing terms: Breakdown and gas discharges, Gas discharges

Abstract: The dual purpose of the present work was first to examine the effect of humidity and gas density on the breakdown characteristics of short airgaps and secondly to investigate whether charge injection data could provide additional information concerning the probability of breakdown at low probability levels. Impulse tests were, therefore, performed in a sealed test vessel using laboratory air for pressures in the range 0.7–1.4 bar and absolute humidity levels from ~2 to 15 g/m^3. Both pressure and humidity could be closely controlled and measured. The impulse shape was +100/2500 μs and the test gap consisted of a 5 cm-diameter sphere at 20 cm above an earthed plane. Statistical flashover tests and measurements of apparent charge injection at the sphere were made and both sets of data were analysed using the method of maximum likelihood. The breakdown probabilities were found to satisfy a normal distribution and the charge measurements provided significant additional information at low probability levels. The measured values of V_{50} were found to depend linearly upon absolute humidity with a slope of 1.5 kV/g/m^3 at all pressures. The withstand voltages, on the other hand, were only weakly dependent upon absolute humidity. The humidity correction factors found in the present work agree well with the IEC standard at 1.2 and 1.4 bar, but depart appreciably at lower pressures.

1 Introduction

The present work is concerned with an investigation of impulse breakdown of laboratory air under carefully controlled conditions. Much interest has been shown in recent years (e.g. CIGRE Working Group 33.03 and Pigini *et al.* [1]) in improving IEC Standards by establishing reliable correction factors for the air density and humidity over the range that is found in naturally occurring situations.

Paper 5718A (S3), first received 21st November 1986 and in revised form 27th July 1987

Dr. Davies, Dr. Turri and Prof. Dutton are with the Department of Physics, University College of Swansea, Swansea SA2 8PP, United Kingdom

Prof. Waters is with the Department of Electrical and Electronic Engineering, UWIST, Cardiff CF1 3XE, United Kingdom

Many of the previous investigations have been in the open or in laboratory air when it is extremely difficult, if not impossible, to control the experimental conditions. The normal procedure is to take measurements over as short as possible a time and to consider average values of the temperature, pressure and humidity over the period of the test. Any test, however, invariably takes some hours to complete and all the above parameters can vary considerably on this time scale. Systematic changes with uncontrolled parameters such as electrode condition, dust pollution and background ionisation are also masked.

To carry out the present investigations, therefore, a sealed system has been constructed in which it is possible to monitor and control closely the gas density and humidity and to make physical measurements of the discharge process. Thus breakdown voltage measurements of sphere–plane gaps subjected to switching impulses have been carried out over the pressure range 0.7–1.4 bar and absolute humidity levels from of order of 2 to 15 g/m^3, and, in order to investigate the effect of humidity on the corona development, simultaneous time-resolved measurements have also been made of the apparent charge injection at the anode. Previous workers [2, 3] have suggested that measurement of some physical parameter, such as the apparent charge injection, as well as providing more quantitative data than conventional breakdown tests, may also enable a criterion to be established for determining the breakdown probability of the gap for a given set of conditions. This hypothesis is further investigated in the present work. Preliminary results have already been reported for dry air [4].

2 Apparatus

The experimental arrangement is shown in Fig. 1 and consists of a sealed all-metal ionisation chamber, of internal height 3 m and internal diameter 1.2 m, connected to a single-stage Marx generator producing positive polarity 100/2500 μs impulse voltages having a maximum crest value of approximately 200 kV. This shape is suggested by the IEC Standards as an alternative to the usual 250/2500 μs shape for switching impulses and has already been employed in other investigations in these laboratories [4, 5].

The chamber was filled with normal laboratory air (which contains the natural amount of CO_2 in contrast to commercial dry air where it is absent) and the pressure could be set and maintained to well within 0.1%. The temperature was continuously monitored and remained constant at 293 ± 1 K.

The humidity control system shown in Fig. 2 consists of a closed loop around which the air is circulated by means of a diaphragm pump having PTFE diaphragms

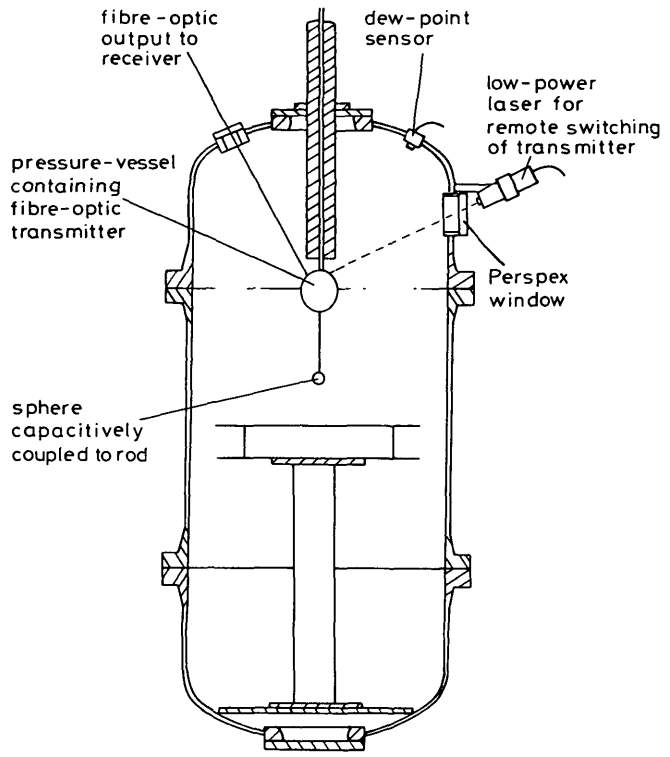

Fig. 1 *Ionisation chamber used in the tests*

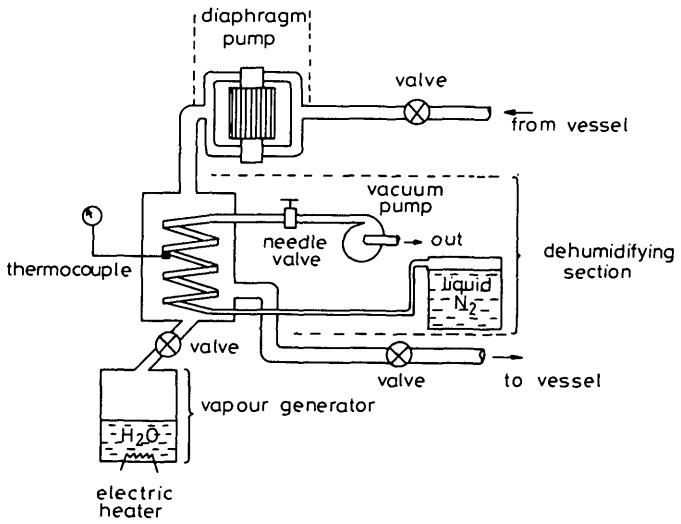

Fig. 2 *Humidity control system*

and *Viton 'O'* rings. Moisture can be removed by cooling a condensing coil with cold nitrogen gas drawn off from a flask of liquid nitrogen. A needle valve inserted in the nitrogen circulation loop allows the temperature of the condensing coil to be controlled to prevent condensation of the natural nitrogen content of the air in the chamber. Alternatively, the moisture level can be increased by boiling off water using an electrically heated coil.

The absolute humidity at a given pressure was determined from the dew point which was measured with a commercial Protimeter dew-point meter having an electrically cooled gold mirror and automatic readout of the dew point, ambient temperature and relative humidity. The dew point is practically independent of pressure (about 0.1% change for 1 bar of pressure variation [6]) and gives a direct measure of absolute humidity. The closed loop control circuit discussed above enabled the conditions inside the vessel to be controlled so as to maintain the dew point constant to within 0.1 K.

The high voltage electrode was a 5 cm-diameter sphere capacitively coupled to the high voltage bushing. The signal developed on the capacitor thus gave a measure of the apparent charge injected and was transmitted to the recording system by a remotely switched fibre-optic link. The cathode was a 1 m-diameter aluminium plane 20 cm below the tip of the sphere.

To ensure that successive impulses were independent of each other, a constant period of two minutes was allowed to elapse between voltage applications during which time a fan was activated in order to help dissipate the space charge left in the discharge space by the previous impulse. It has previously been observed [7] in similar conditions, and in a chamber of comparable volume, that at atmospheric pressure the negative-ion density left by a corona discharge has practically returned to normal levels after a two minute interval.

3 Breakdown probability: analysis of flashover data

In the investigation of the breakdown characteristics a standard multilevel test procedure was adopted where, for each pressure and humidity level considered, 20 impulses were applied at up to seven crest voltages. At each voltage level, the number of breakdowns was recorded together with the time-to-breakdown and the apparent charge injection for each individual impulse.

The flashover data were analysed on the assumption that the probability of breakdown $P_B(V)$ corresponding to a crest voltage V satisfied a cumulative normal distribution:

$$P_B(V) = \frac{1}{\sqrt{2\pi}\,\sigma} \int_{-\infty}^{V} \exp\left[-(V - V_{50})^2/2\sigma^2\right] dV \qquad (1)$$

with the parameters V_{50} (i.e. the crest voltage for which there is a 50% probability of breakdown) and σ being estimated using the likelihood analysis as described in a companion paper [8]. Other workers have suggested that other distributions, such as the *Weibull* or *Gumbell* distribution, might be more appropriate at low breakdown probability levels but they are indistinguishable from the cumulative normal distribution at the probability levels relevant to the present work (>2%).

Figs. 3*a–d* show the results of the likelihood analysis, i.e. the maximum likelihood estimates of V_{50} and σ together with the 90% confidence region for the simultaneous estimates of the two parameters and the 90% confidence intervals for their individual estimates. Note that the 90% confidence region has a 90% probability of including the true values of both V_{50} and σ whereas the 90% confidence interval for a single parameter has a 90% probability of including the true value of that parameter with the second parameter remaining undetermined. For a full discussion, see [8].

Each data set corresponding to a given pressure and humidity level was subjected to a χ^2 test and values of χ^2/γ, where γ is the number of degrees of freedom ($=N-2$ where N is the number of voltage levels), are also reported in the figure captions. Values of χ^2/γ considerably greater than unity indicate that either the particular data is not consistent with a cumulative normal distribution or that there may be some inconsistency in the data. We see, for example, that the data set for 0.8 bar and absolute humidity of 15.5 g/m^3 (Fig. 3*a*) has $\chi^2/\gamma = 4$

so that care should be taken in drawing any conclusion from the results of that particular test. This is also reflected in the very large confidence region associated with V_{50} and σ.

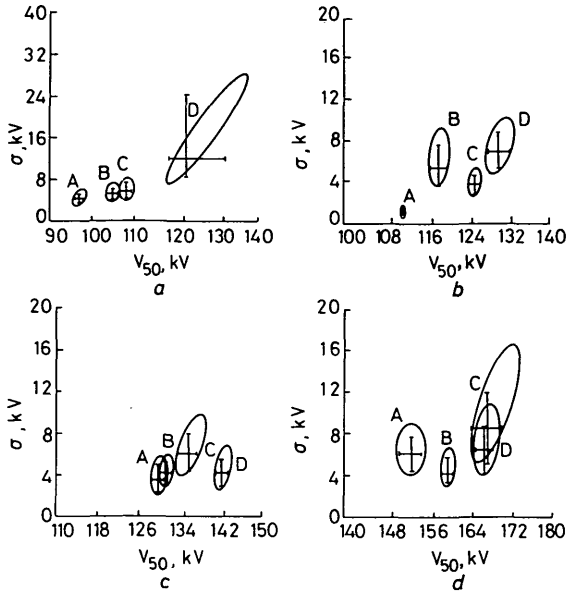

Fig. 3 *Maximum likelihood estimates of V_{50} and σ together with elliptical 90% confidence regions for the simultaneous estimates of these parameters*

Pressure bar	A		B		C		D	
	Absolute humidity, g/m³	χ^2/γ	Absolute humidity, g/m³	χ^2/γ	Absolute humidity, g/m³	χ^2/γ	Absolute humidity g/m³	χ^2/γ
0.8	2.7	0.5	6.7	0.3	9.1	1.2	15.5	4.0
1.0	2.1	0.3	8.0	1.2	11.5	2.1	14.8	0.4
1.2	2.7	2.3	6.7	0.9	10.0	1.0	13.9	0.6
1.4	2.4	0.9	6.6	0.6	10.0	0.3	15.0	0.2

a $p = 0.8$ bar
b $p = 1.0$ bar
c $p = 1.2$ bar
d $p = 1.4$ bar
The bars on the vertical and horizontal lines define 90% confidence intervals for the individual parameters

From Figs. 3*a–d* it can be noted that the estimates of V_{50} have quite narrow confidence intervals while the estimates of σ are often associated with large confidence intervals (in per-unit terms) which indicates that the estimation of σ is not so accurate as V_{50} as is well known in high-voltage testing.

For each pressure and humidity level at least one voltage level resulted in a zero frequency of breakdown. Although the maximum likelihood method allows these data to be utilised if required, they may have the effect of biasing the maximum likelihood estimate of σ. This may be seen in Figs. 4*a–d* which show the test data and the corresponding normal distributions determined from the maximum likelihood analysis (i) including all the test data and (ii) excluding those cases where no breakdown were observed.

In simple graphical fitting of probability curves to test data, it is not possible to take a quantitative account of data points for the zero breakdown frequency cases since these should be situated at infinity on the vertical axis of the normal probability paper. Nevertheless, it can be seen that the inclusion of such points would tend to increase the slope of the distribution (i.e. σ decreases) without appreciably changing V_{50}.

In the test series, each set of measurements is a binomial trial from an infinite population and, denoting the true probability of breakdown at a given level by P, the confidence interval for the observed breakdown frequency P_m (i.e. the number of breakdowns divided by the

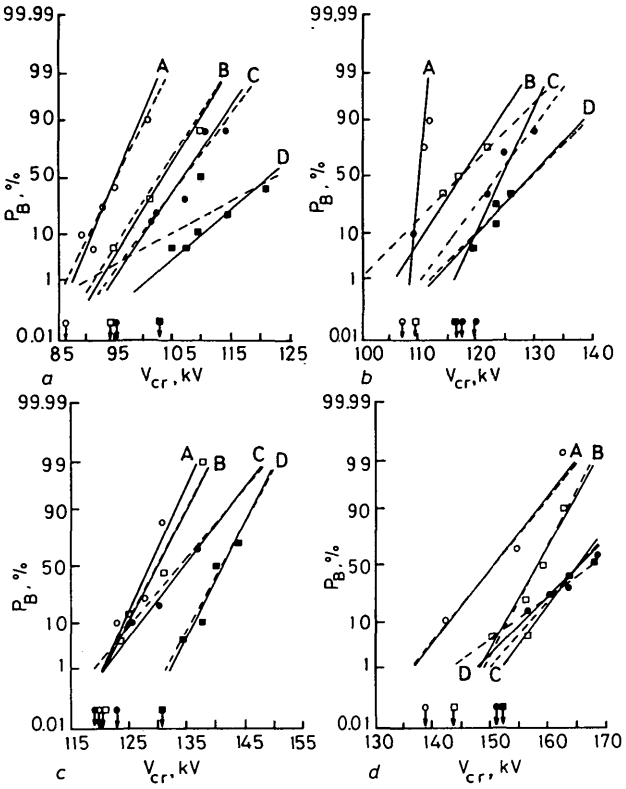

Fig. 4 *Plots on normal probability paper of the test data and corresponding normal distributions determined using the method of maximum likelihood*

——— includes all test data
– – – – excludes cases where no breakdowns were observed
The absolute humidities as in Fig. 3
a $p = 0.8$ bar
b $p = 1.0$ bar
c $p = 1.2$ bar
d $p = 1.4$ bar

total number of shots) is given by

$$P_m \pm z\sqrt{\frac{P(1-P)}{N}} \tag{2}$$

where N is the total number of impulses at a given level and z is a coefficient which depends on the desired confidence level and can be found from standard tables. Typical values of z are shown in Table 1.

Since the true value P of the breakdown probability is unknown the confidence intervals are estimated from eqn. 2 with P replaced by P_m, which will obviously be more accurate the larger N.

Table 1: Values of parameter z in eqn. 2 corresponding to various confidence levels

Confidence level	z
99%	2.58
95%	1.96
90%	1.64
80%	1.28

In the IEC standard tables [9] it is suggested that $N = 20$ is a good compromise between the number of voltage applications and an acceptable confidence interval and this was the value adopted in our present work.

For low breakdown probabilities, however, the lower limit of the confidence interval can extend to very small

values and in fact will be zero when

$$P_m = z\sqrt{\frac{P_m(1 - P_m)}{N}} \tag{3}$$

i.e.

$$P_m = \frac{z^2}{N + z^2} \tag{4}$$

which is shown in Fig. 5 for the case of $z = 1.64$ corresponding to a 90% confidence level. It can be seen, for example, that for $N = 20$ all measured frequencies of

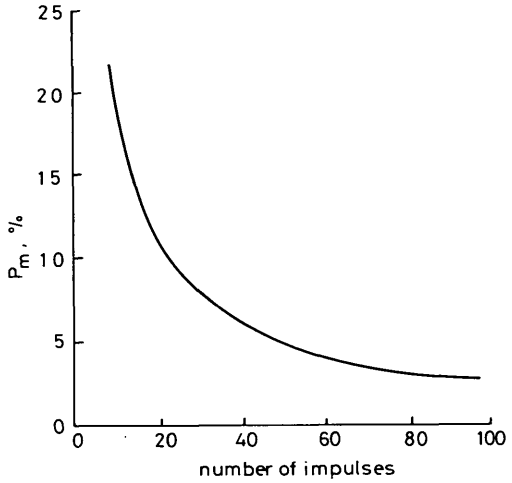

Fig. 5 *Values of observed breakdown frequency P_m for which the lower limit of the 90% confidence interval for P_m is equal to zero, plotted against number of impulses in a test series*

breakdown less than 11% will have lower confidence limits which extend to infinity on probability paper. To obtain an acceptable confidence interval it would be necessary to increase the number of shots in the series as the voltage level decreases. Even for quite moderate probability levels, of the order of 1%, the number of shots required becomes very large ($\sim$300 shots to give a finite lower limit).

It should be noted that an accurate estimate of both a low breakdown probability voltage level (such as V_1) and V_{50} means that the whole breakdown probability distribution would be determined (on the assumption that a given two-parameter distribution such as the cumulative normal distribution is appropriate). This should be regarded as a particular case of the more general problem that unless a very large number of impulses is employed it is not possible to determine both parameters of a two-parameter breakdown probability distribution with good confidence intervals, solely from flashover data (i.e. a binomial trial of breakdown or withstand).

The confidence intervals associated with each parameter will depend upon the testing strategy chosen. For example, the standard up-and-down technique will give a good estimate of V_{50} but will result in a large confidence interval for σ. Both parameters, however, need to be determined accurately if it is desired to extrapolate to evaluate the breakdown probability at voltages corresponding to high or low probability levels (the extrapolation procedure would still of course be dependent upon determining the correct distribution).

It has been pointed out previously [2, 3] that the amount of information in a statistical test series can be greatly enhanced if some physical parameter, such as current, charge or energy injection, is measured in addition to observing whether breakdown does or does not occur. Provided that the parameter measured can be related to the probability of breakdown then fewer shots would be needed to determine, for example, voltage levels corresponding to low breakdown probabilities. The additional information provided by physical data can also be helpful in identifying causes of the abnormal probability distributions that have often been observed (see, for example, Reference 10).

For this reason time-resolved measurements were made of the apparent charge injection from the spherical anode, both to determine whether that quantity would be suitable for determining the breakdown probability and also to give a measure of the injected space charge and its dependence on humidity and gas density.

4 Analysis of corona charge injection measurements

The apparent charge injection signal measured at the high voltage electrode consists of several components, each one corresponding to a different phase of the discharge.

Considering the two typical shots of Fig. 6 (withstand and breakdown, respectively), the typical signal can be subdivided into the following components:

q_g is the capacitive charge due to the geometric field

q_1 is the fast increase (almost instantaneous on this timebase) corresponding to the first corona development

q_2 (q_3, q_4, ...) are the subsequent primary corona

Q_I is the total charge injected during the primary corona (equal to $q_1 + q_2 + q_3 + \ldots$)

q_s is the continuous, stepped increase of the signal which is much slower than the primary corona charge injection (hundreds of microseconds compared with hundreds of nanoseconds)

q_t is the total charge injection, i.e. the maximum amplitude of the signal minus q_g.

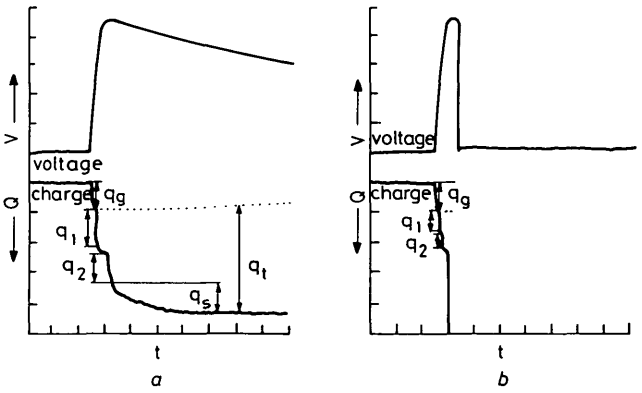

Fig. 6 *Typical oscillograms of applied voltage and apparent charge injection at the anode*

a A withstand event
b A breakdown
The broken line indicates the apparent charge injection induced by the applied electric field

In the case of breakdown, the voltage collapse occurs either in coincidence with one of the primary corona (usually the second) or during the continuous stepped increase q_s. In previous work [11], the phase corresponding to q_s was referred to as 'secondary corona' because the light emitted from the discharge, recorded by a photomultiplier, showed a train of small impulses in

phase with these stepped charge increments. In the case of breakdown direct from the primary corona without a clear secondary corona sequence being present, it is likely that the onset of an unstable secondary phase leads directly to breakdown.

In the primary corona sequence it was noteworthy that, for all pressures and absolute humidities, an inverse relationship existed between the first and subsequent primary corona; i.e. the greater the charge injected during the first corona q_1 the smaller the charge injected during the subsequent corona $q_2 + q_3 + \ldots$. Indeed if q_1 was large enough no subsequent primary corona events were observed. This is due to the distortion of the electric field distribution, which is reduced near the electrode and in the space charge zone almost in proportion to the injected charge. Because of this field reduction subsequent corona have to propagate initially in a lower field region, even though further into the gap the field is enhanced [12].

It was also found that the total charge injected during the primary corona Q_I was almost constant for fixed applied voltage, pressure and humidity.

Fig. 7 shows the total average corona charge $\bar{Q}_I$ as a function of crest voltage at four different pressure levels.

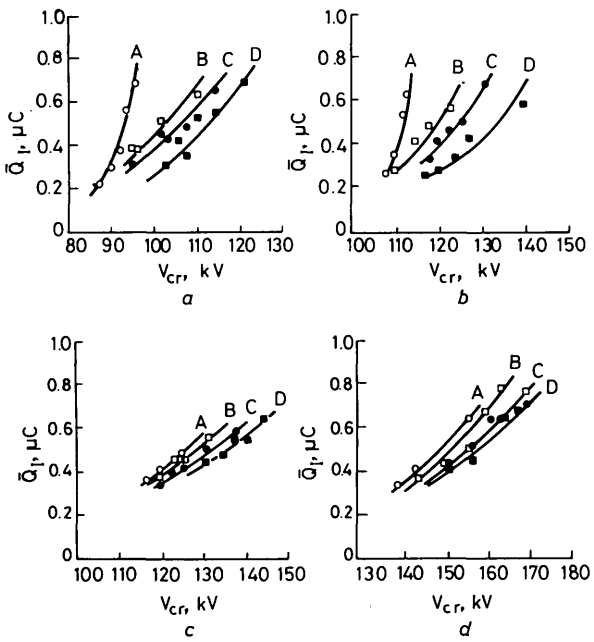

Fig. 7 *Total apparent charge injection at anode during primary corona (averaged over 20 shots) against crest voltage*
Absolute humidities as in Fig. 3
a p = 0.8 bar
b p = 1.0 bar
c p = 1.2 bar
d p = 1.4 bar

$\bar{Q}_I$ was averaged over the 20 shots forming a set of measurements and the percentage standard deviation was found in all cases to lie between 10 and 20%. We see that at fixed pressure and humidity levels $\bar{Q}_I$ increases rapidly with the crest voltage (the lines in Fig. 7 have only been drawn to indicate the trend of the data). At a given voltage level there is a considerable decrease of $\bar{Q}_I$ as the humidity content increases. This effect is more marked at lower pressures which implies that the relative water content per unit mass of air is significant and that the presence of water vapour strongly inhibits corona development.

In the present work the charge injection during the primary corona sequence has been selected for study because it is the first phase of the discharge process and thus should greatly influence the subsequent discharge development. Furthermore, it is a parameter which is almost always measurable both in withstand and breakdown events (see Fig. 6), so that the statistical analysis can be based on all the 20 shots forming a set of measurements.

5 Breakdown probability: combined analysis of charge injection and flashover data

We have seen that by varying the humidity content both the probability of breakdown and the average primary corona charge injection ($\bar{Q}_I$) can vary considerably. The observations also show that, with other parameters fixed, $\bar{Q}_I$ is uniquely related to the crest voltage. We may therefore, for a given set of conditions, attempt to determine the breakdown probability distribution associated with a given $\bar{Q}_I$, again assuming that the cumulative normal distribution applies.

In Fig. 8 the same experimental data shown in Fig. 4 are used to plot the measured frequencies of breakdown

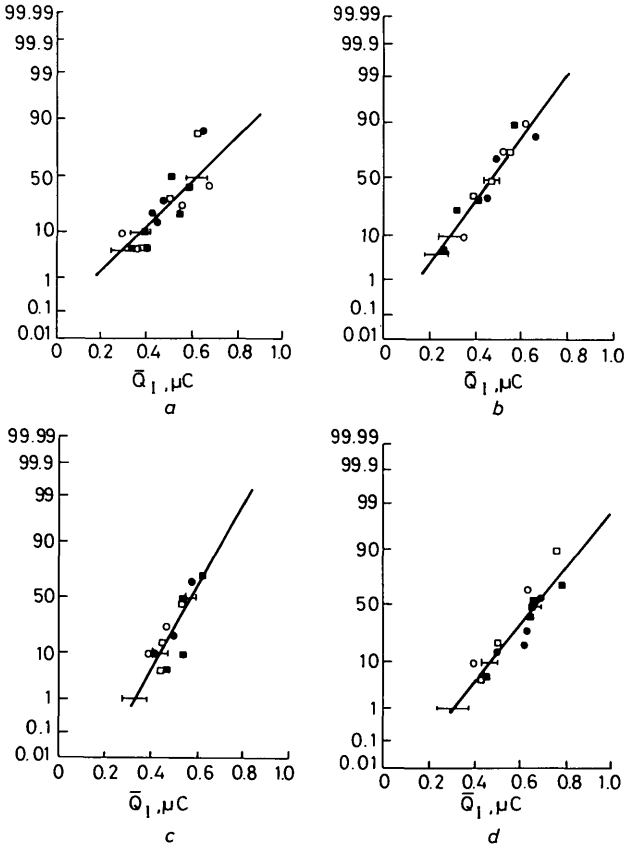

Fig. 8 *Measured breakdown frequencies plotted on normal probability paper against the average total charge injection $\bar{Q}_I$ during the primary corona together with the corresponding normal distributions estimated using the method of maximum likelihood*
Absolute humidities as in Fig. 3
a p = 0.8 bar ○ = A
b p = 1.0 bar □ = B
c p = 1.2 bar ● = C
d p = 1.4 bar ■ = D

on normal probability paper as a function of the measured $\bar{Q}_I$ for the four pressure levels considered and humidities in the range 2–15 g/m^3. Only data sets having a breakdown frequency between 5% and 95% were considered, i.e. sets where at least either one collapse or one withstand of the test gap was observed in 20 successive

impulse applications. It can be seen that at each pressure level the corona charge injection data at different humidities overlap and appear to define a unique breakdown probability distribution that is practically independent of humidity. The 'likelihood analysis' was thus applied to the charge injection data in order to estimate the parameters of the corresponding breakdown probability/charge distribution, and the results were used to plot the straight lines in Fig. 8*a–d* where the horizontal bars indicate the 90% confidence intervals at probability levels of 50, 10 and 1%, respectively (the confidence intervals have been computed as in Reference 8).

The above result is of particular importance for the following reasons:

(*a*) It strongly suggests that, at a given pressure, $\bar{Q}_I$, although varying considerably with the humidity level and applied voltage (Fig. 7), is directly related to the probability of breakdown. Variations in the water vapour content do not alter this relationship but will only change the value of the applied voltage needed to obtain a certain $\bar{Q}_I$ (and therefore a certain probability of breakdown).

(*b*) The average charge injection/breakdown probability distributions can be determined on the basis of a much greater number of shots since there is no need to distinguish between data corresponding to different humidity levels.

(*c*) The additional information that $\bar{Q}_I$ gives about the probability of breakdown may be used in the determination of the crest voltage/breakdown probability distribution. In particular, it is possible to assign a finite breakdown probability to voltage levels where no breakdowns (out of twenty shots) were observed and which, in the conventional method of graphical fitting on probabilistic paper, would be estimated at infinity (we have already pointed out in Section 3 how these particular data could bias the estimation of the parameters of the distribution). Care must be taken, however, not to extrapolate to very low probability levels (lower than of order 1–2%) since there is no proof that the cumulative normal distribution, or any other distribution, will hold at these levels.

The likelihood analysis of Section 3 was thus repeated incorporating the extra information given by $\bar{Q}_I$ at the low probability levels (for which the measured breakdown frequency was zero) and it was found that, while V_{50} was practically unchanged, the new estimates of σ differed considerably from those obtained previously in thirty to forty percent of the cases considered. The new estimated parameters, however, were always within the 90% confidence regions of Figs. 3*a–d*.

The results of the combined statistical analysis are shown in Figs. 9*a–d*, plotted on probability paper since this allows direct comparisons to be made between the different distributions, estimated using the generalised likelihood method, and the experimental data. The actual values of V_{50}, σ and corresponding 90% confidence intervals are shown in Fig. 10 and Fig. 11 of Section 6. The arrowed symbols in Figs. 9*a–d* indicate that for these points, since the measured breakdown frequency was zero, the probability of breakdown deduced from $\bar{Q}_I$ (Fig. 8) has been used.

If we compare the results of Figs. 4*a–d*, based on flashover data only, with those of Figs. 9*a–d* (combined analysis), we see that in the latter case more consistent distributions are estimated, i.e. σ increases monotonically with absolute humidity which is in line with the general trend of small values of σ at low humidity and high values at high humidity.

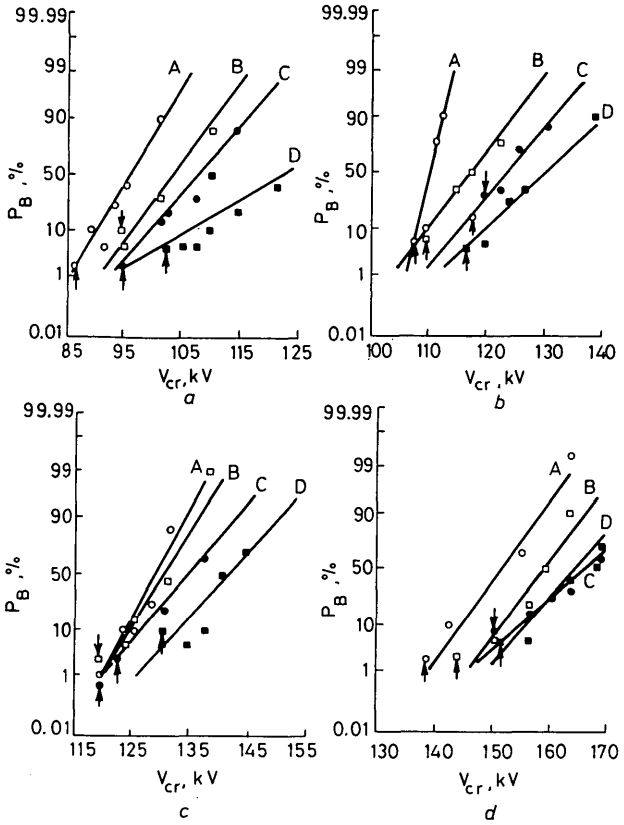

Fig. 9 *Results of the combined statistical analysis*

Arrowed symbols indicate that the breakdown probability has been estimated from the charge injection data

Absolute humidities as in Fig. 3

a p = 0.8 bar

b p = 1.0 bar

c p = 1.2 bar

d p = 1.4 bar

Although we have estimated the breakdown frequency from $\bar{Q}_I$ only for those measurements where the observed breakdown frequency was zero, it is also possible to carry out the same procedure for all the measurements. If this is done, the resulting crest voltage/breakdown probability distributions are unchanged.

Finally, for completeness, the combined analysis was repeated for several data sets assuming a symmetric *Weibull* distribution, as used by Carrara and Yakov [13], both for the voltage and charge breakdown probability distributions. The results were almost identical to the above, which is not surprising since the *Weibull* distribution is very close to the normal cumulative distribution for probabilities greater than 2%.

6 Influence of humidity and gas density on the breakdown characteristics

From the likelihood analysis of Figs. 3*a–d* and the breakdown probability distributions of Figs. 9*a–d* it can be easily seen that an increase of the humidity level and/or gas density both result in an increase in the 50% breakdown voltage. This is a commonly observed behaviour of airgaps [12, 14], at least for small values of $p \times d$ where the breakdown occurs through a streamer mechanism. The different mechanisms by which humidity and density influence the dielectric strength of the gas are, however, not very well understood. In the present investigation, therefore, a large amount of flashover data were

obtained, with the two parameters varied independently, in order to quantify experimentally their different effects.

Fig. 10 shows the variation of V_{50} with absolute humidity together with the 90% confidence intervals as estimated from the generalized likelihood ratio [8]. We see that the increase of V_{50} with absolute humidity in this test gap may be taken to be linear at all pressures considered with approximately constant slope of 1.5 kV per g/m^3.

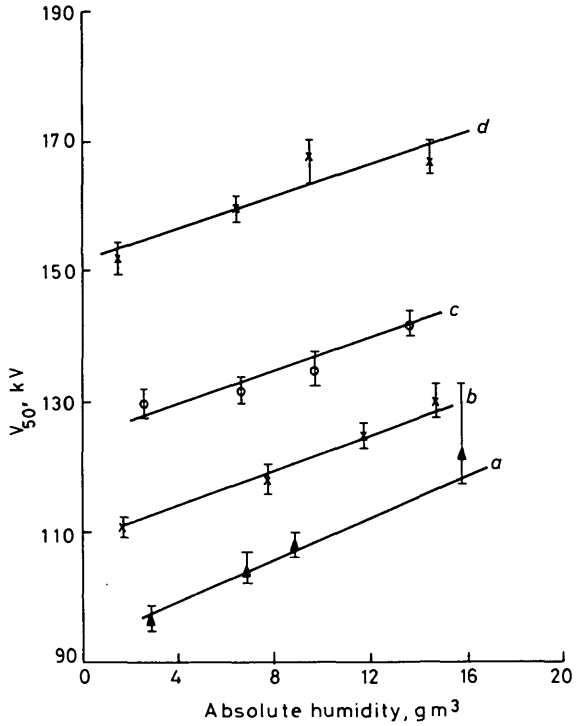

Fig. 10 *Variation of V_{50} with absolute humidity at various pressures*
The barred vertical lines are the 90% confidence intervals for V_{50}

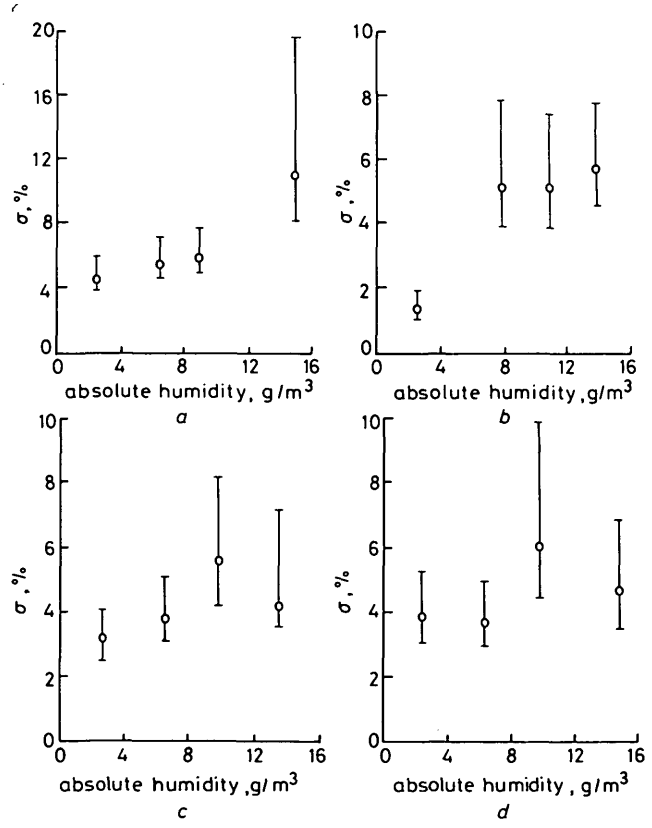

Fig. 11 *Variation of σ with absolute humidity at various pressures*
The barred vertical lines are the 90% confidence intervals for σ
a p = 0.8 bar
b p = 1.0 bar
c p = 1.2 bar
d p = 1.4 bar

Figs. 11*a–d* show the corresponding variation of σ and its associated 90% confidence intervals. We observe that even though the confidence intervals are quite large, an increase of σ with absolute humidity is seen at 0.8 and 1.0 bar and the trend is still present at 1.2 and 1.4 bar although not so precisely defined (this trend corresponds to the decreasing slope of the straight lines in the probability distributions of Figs. 9*a–d* as the humidity increases).

This is an indication that the presence of water vapour tends to increase the statistical dispersion of the data and it is this increase in the dispersion which is the main factor involved in the enhancement of V_{50}, particularly at lower pressures.

This has the important implication that, despite the increase of V_{50}, the inherent dielectric strength of the gas is not necessarily increased. In fact, at voltages corresponding to low probability levels, e.g. V_5, the increase of V_5 with absolute humidity is much less pronounced than V_{50}. Indeed extrapolation of the distributions in Figs. 9*a–d* indicates that the voltage level corresponding to a breakdown probability of about 0.1% does not depend upon the humidity level. Our present results thus show that, for a fixed gas pressure, whereas V_{50} varies strongly, the withstand voltage is practically constant or very weakly dependent on humidity.

On the other hand, as is well known, if the gas density is increased, a real improvement in the dielectric strength is achieved since both V_{50} and the withstand voltage increase.

The separate effects of humidity and gas density are well illustrated by the fact that V_{50} at 1.0 bar and 14.8 g/m^3 has the same value (130 kV) as that measured at 1.2 bar and 2.7 g/m^3 (see Figs. 9*b* and 9*c*). Because of the different values of σ, however, the voltage level corresponding to 1% breakdown probability in case (*a*) is 113 kV compared with 122 kV in case (*b*), i.e. 9 kV lower.

For the conditions of the present investigation, the IEC Standard humidity correction factor, k_h, (relating the measured V_{50} to the value of V_{50}, referred to a standard absolute humidity level of 11 g/m^3), is given by the dashed curve of Fig. 12 [9]. These values of k_h are independent of pressure according to the Standards. On the other hand, values of k_h evaluated from our present measurements, also plotted in Fig. 12, show considerable Variation from the Standard and a strong pressure dependence. This would indicate that an extensive further programme is necessary to obtain systematically reliable correction factors for different gas pressures, electrode geometries and applied voltage shapes.

To see the effect of gas density on the breakdown voltage, four additional data sets were taken at low absolute humidity at pressures of 0.7, 0.9, 1.1 and 1.3 bar. From Fig. 13 we see that V_{50} increases nonlinearly at low pressures, but for pressures above about 1.0 bar, tends asymptotically to a slope of 110 kV bar^{-1} at low absolute humidity and 120 kV bar^{-1} at high humidity. We note that in open laboratory experiments, with variable humidity, V_{50} would lie somewhere between those curves and there would be an increase in the statistical spread of the results leading to large confidence intervals. In addition, without controlling the humidity, it would be very difficult to define the form of the curves.

The reduced average applied field E_{50}/p ($= V_{50}/pd$) is

shown as a function of pressure in Fig. 14. We see that above 1.0 bar E_{50}/p tends to constant values of 5.5 kV cm^{-1} bar^{-1} at low humidity, and 6 kV cm^{-1} bar^{-1} at high humidity, which is comparable with the minimum reduced electric field necessary for a stable streamer propagation in non uniform fields in dry air [12].

The nonlinear increase of V_{50} with pressure (Fig. 13) strongly resembles the breakdown characteristic measured in previous work [15], again for a 5 cm diameter spherical anode and plane cathode, but with various gap spacing in open laboratory air. This electrode geometry was specifically chosen to investigate the transition regime between quasiuniform and nonuniform field breakdown and it was found that for d greater than 20 cm (the pressure level was 1.0 bar) the transition to nonuniform field breakdown was complete, and that V_{50} increased linearly with d at a rate of 5.5–6 kV cm^{-1}.

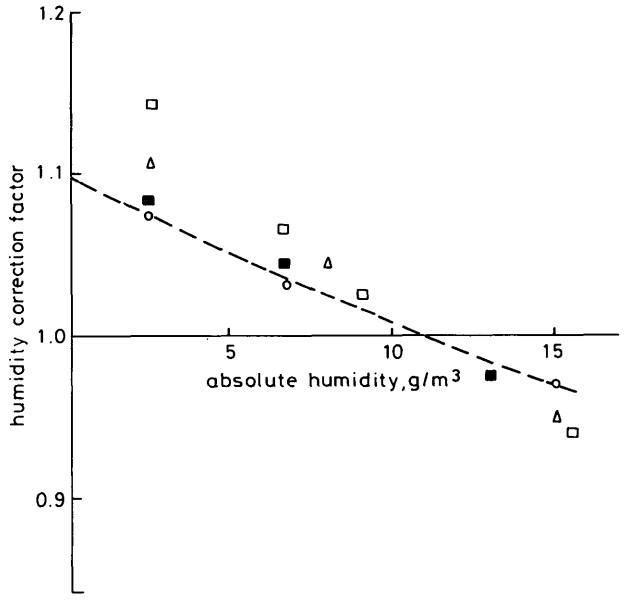

Fig. 12 *Comparison of the humidity correction factors found in the present investigation at various pressures with the IEC standard correction factors*

Pressures: □ = 0.8 bar
△ = 1.0 bar
■ = 1.2 bar
○ = 1.4 bar
- - - IEC Standard

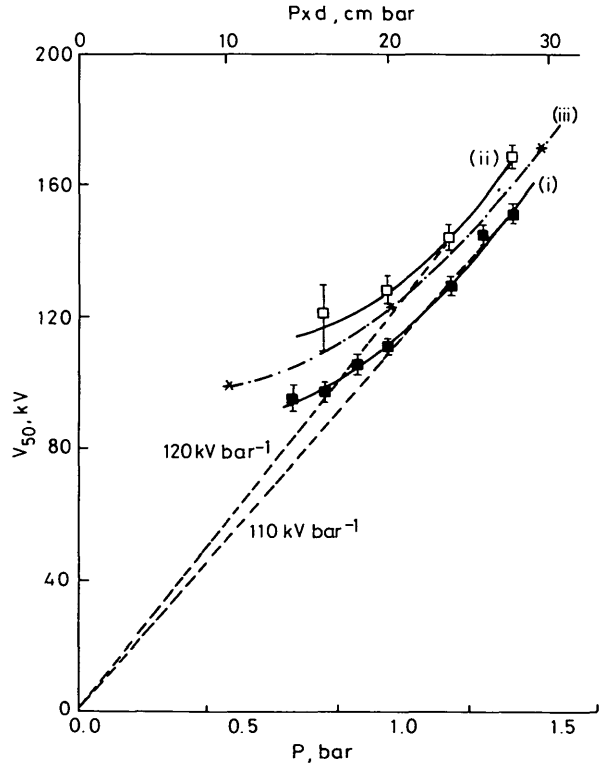

Fig. 13 *Variation of V_{50} with pressure at 2.7 g/m^3 (■) and 15.0 g/m^3 (□) together with previous measurements by Davies et al. (×) in open laboratory air at various gap distances plotted against pd [15]*

The barred vertical lines indicate the 90% confidence intervals

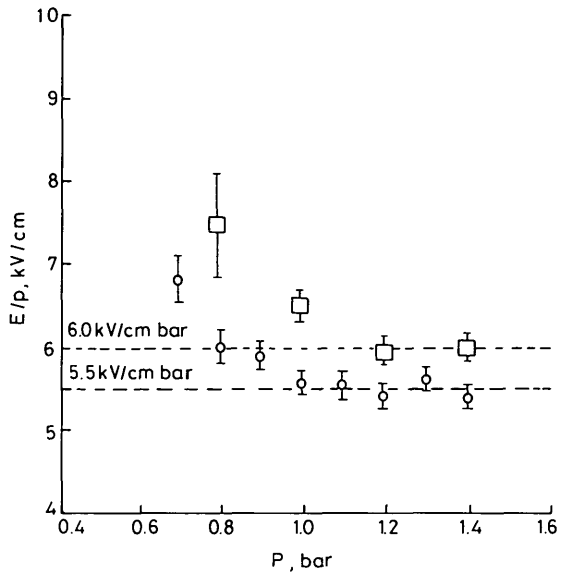

Fig. 14 *Reduced average applied field E_{50}/p ($=V_{50}/pd$) against pressure at high and low absolute humidity levels*

The barred vertical lines indicate the 90% confidence intervals
○ = 2.7 g/m^3; □ = 15 g/m^3

With regard to the horizontal $p \times d$ axis of Fig. 13, our present results are consistent with the previous measurements (curve (iii) in Fig. 13), bearing in mind that in these the humidity was not controlled and could have varied considerably during the investigation.

Fig. 15 shows the variation of σ with pressure at low humidity (~2.5 g/m^3) together with the 90% confidence intervals. We see that σ is a minimum at about 1 bar, increases slowly at higher pressures and rapidly at lower pressures, corresponding to the transition regime of

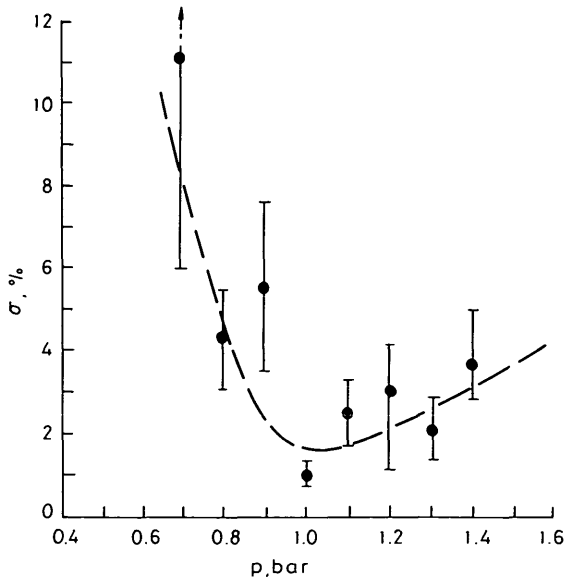

Fig. 15 *Variation of σ with pressure at low absolute humidity (~2.5 g/m^3)*

The barred vertical lines indicate the 90% confidence interval of σ

Fig. 13. In previous work [16] with lightning impulse shapes, the complete transition of the breakdown characteristic was followed from quasiuniform to nonuniform field breakdown, and in that work a big increase was also found in the standard deviation of V_{50} in the transition region.

The average primary corona charge injection $\bar{Q}_{I50}$ at the voltage level V_{50} may be found from Figs. 8*a–d*, and is shown as a function of the pressure in Fig. 16 together

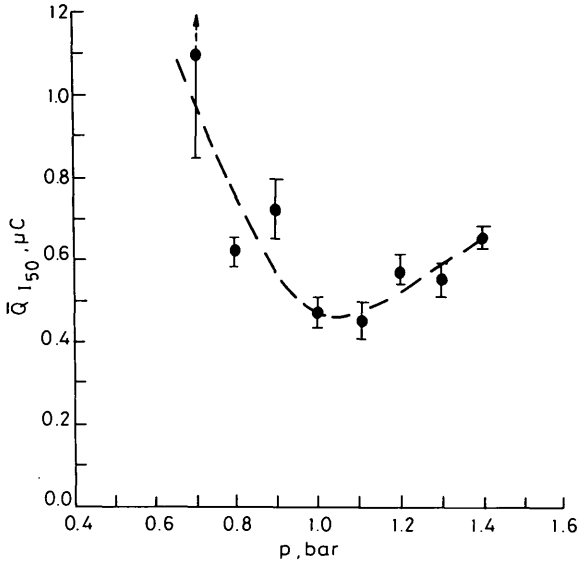

Fig. 16 *Average charge injection $\bar{Q}_{I50}$ during the primary corona at a voltage level V_{50} against pressure*

The vertical barred lines indicate the 90% confidence interval for $\bar{Q}_{I50}$

with the additional data obtained at low humidity at pressures of 0.7, 0.9, 1.1 and 1.3 bar. We note that $\bar{Q}_{I50}$ varies in a very similar manner to σ, having a minimum at about 1.0 bar and increasing markedly at pressures below 1.0 bar.

7 Conclusions

A systematic investigation has been carried out, for a sphere/plane gap in laboratory air subjected to positive switching impulses, of the breakdown characteristics and apparent charge injection for a range of air densities and humidity levels that occur naturally in temperate climates. Work is also in progress to extend the measurements to absolute humidities of order 30 g/m^3 to investigate behaviour relevant to tropical climates.

The results indicate that the apparent charge injection, Q_I, during the primary corona phase, is directly related to the probability of the subsequent breakdown, the associated breakdown probability/charge distribution being practically independent of the humidity level. This enables further information to be gained concerning the breakdown probability for applied voltage levels where no breakdowns are observed in a standard multilevel test. A combined analysis, based on both flashover and charge injection data, appears to be a satisfactory alternative to greatly increasing the number of shots at low probability levels in binomial flashover tests.

For the statistical analysis of the data a *generalized maximum likelihood* method was used which enabled the parameters of the breakdown probability distributions to be estimated together with the corresponding confidence intervals.

The test data appear to satisfy the cumulative normal distribution specified by the parameters V_{50} and σ and the analysis indicates that

(*a*) V_{50} increases almost linearly with absolute humidity with a slope of about 1.5 kV per g/m^3 at all pressure levels

(*b*) σ also increases with absolute humidity but this effect is more marked at pressure of order or lower than 1.0 bar

(*c*) the withstand voltage appears to be only weakly dependent on absolute humidity.

The humidity correction factors derived from our present results are pressure dependent and, although in good agreement with the IEC Standard at pressures of order 1.4 and 1.2 bar, differ appreciably as the pressure decreases.

The variation of V_{50} with pressure is nonlinear and is consistent with measurements obtained in our previous work where the transition regime from quasiuniform to nonuniform field breakdown was investigated. At pressures above 1.0 bar V_{50} appears to increase linearly with p corresponding to constant reduced fields of order 5.5 and 6 kV/cm bar at low and high absolute humidity, respectively.

Below 1.0 bar, i.e. in the transition region, the reduced field necessary for a 50% breakdown probability increases rapidly and is associated with rapid increases in σ and the apparent charge injection.

8 Acknowledgments

This work has been carried out with the aid of a Research Grant GR/B/4892.5 from the UK Science and Engineering Research Council. We are grateful to members of the EEC Group on Energy Exchange Processes in Electrical Discharges for much helpful discussion.

9 References

1 PIGINI, A., SARTORIO, S., MORENO, M., RAMIREZ, M., CORTINA, R., BRITTEN, A.C., and SADURSKI, K.J.: 'Influence of air density on the impulse strength of external insulation', *IEEE Trans.*, 1985, **PAS-104**, pp. 2888–2900

2 BRAMBILLA, R., GARBAGNATI, E., BERTAZZI, A., GALLUCCI, F., and PIGINI, A.: 'Switching impulse tests at very low probability levels'. Proc. 8th Int. Conf. on Gas discharges and their applications, Oxford, 1985, pp. 360–363

3 GELDENHUYS, H.J., LE ROUX, B.C., and MEAL, D.V.: 'Critical charge and critical leader lengths as a means of determining low breakdown probability in large air gaps', *Ibid.*, pp. 352–355

4 DAVIES, A.J., DUTTON, J., TURRI, R., JARVIS, J., ROBLEDO-MARTINEZ, A., and WATERS, R.T.: 'Charge measurements and the determination of low breakdown probabilities in large air gaps'. Proc. 8th Int Conf on Gas Discharges and Their Applications, Oxford, 1985, pp. 356–359

5 DAVIES, A.J., DUTTON, J., SELIM, E.O., and WATERS, R.T.: 'Impulse breakdown of sphere gaps in dry air at pressures in the range one quarter to two atmospheres'. Proc XVI Int. Conf. on Phenomena in Ionised gases (ICPIG), Dusseldorf, 1983, pp. 116–117

6 GLASSTONE, S.: 'Textbook of Physical Chemistry', 1951, MacMillan, London, p. 446

7 POLI, E.: 'Positive corona inception under variable humidity conditions'. Proc. 8th Int. Conf. on Gas discharges and their applications, Oxford, 1985, pp. 593–596

8 DAVIES, A.J., ROWLANDS, A., TURRI, R., and WATERS, R.T.: 'Statistical analysis of flashover data using a generalised likelihood method', *IEE Proc. A*, 1988, **135**, (1), pp. 79–87

9 'High Voltage Test Techniques. Part 2: Test Procedures', International Electrotechnical Commission Publication IEC 60-2, 1973

10 MENEMENLIS, C., and HARBEC, G.: 'Particularities of air insulation behaviour', *IEEE Trans.*, 1976, **PAS-95**, pp. 1814–1821
11 DAVIES, A.J., DUTTON, J., JARVIS, J., ROBLEDO-MARTINEZ, A., and WATERS, R.T.: 'Corona inception, breakdown and charge-injection measurements in sphere-plane gaps subjected to impulse voltages'. Proc. 4th Int. Symp. on Gaseous Dielectrics, Knoxville, 1984
12 GALLIMBERTI, I.: 'The mechanism of long spark formation', *J. Physique*, 1979, **40**, pp. 193–250
13 CARRARA, G., and YAKOV, S.: 'Statistical evaluation of dielectric test methods', CESI Technical Issue, L'Energia Elettrica No. 1, 1983
14 WATERS, R.T.: 'Breakdown in non-uniform fields', *IEE Proc. A*, 1981, **128**, (4), pp. 319–325
15 DAVIES, A.J., DUTTON, J., SELIM, E.O., and WATERS, R.T.: 'The influence of electrode geometry and gas conditions on breakdown processes in the transition from quasiuniform to nonuniform field breakdown'. Proc. 7th Int. Conf. on Gas Discharges and Their Applications, London, 1982, pp. 143–146
16 BYE, P., DAVIES, A.J., DUTTON, J., and WATERS, R.T.: 'Transition regime from quasiuniform to nonuniform field sparkover'. Proc. 4th Int. Conf. on Gas Discharges and Their Applications, IEE, Swansea, 1976, pp. 137–140